





Article

Thermal Properties of Hydrated Lime-Modified Asphalt Concrete and Modelling Evaluation for Their Effect on the Constructed Pavements in Service

Azedin Al Ashaibi ¹, Yu Wang ^{1,*} , Amjad Albayati ^{2,*} , Juliana Byzyka ¹ , Miklas Scholz ^{1,3,4}  and Laurence Weekes ¹

- ¹ School of Science, Engineering and Environment, The University of Salford, Salford M5 4WT, UK; a.a.i.h.alashaibi@edu.salford.ac.uk (A.A.A.); j.byzyka@salford.ac.uk (J.B.); miklas.scholz@tvr1.lth.se (M.S.); l.weekes@salford.ac.uk (L.W.)
 - ² Department of Civil Engineering, University of Baghdad, Baghdad 10071, Iraq
 - ³ Department of Civil Engineering Science, School of Civil Engineering and the Built Environment, University of Johannesburg, Johannesburg 2092, South Africa
 - ⁴ Department of Town Planning, Engineering Networks and Systems, South Ural State University, 454080 Chelyabinsk, Russia
- * Correspondence: y.wang@salford.ac.uk (Y.W.); a.khalil@uobaghdad.edu.iq (A.A.)

Abstract: Flexible pavements are subjected to three main distress types: fatigue crack, thermal crack, and permanent deformation. Under severe climate conditions, thermal cracking particularly contributes largely to a considerable scale of premature deterioration of pavement infrastructure worldwide. This challenge is especially relevant for Europe, as weather conditions vary significantly throughout the year. Hydrated lime (HL) has been recognized as an effective additive to improve the mechanical properties of asphalt concrete for pavement applications. Previous research has found that a replacement of conventional limestone dust filler using hydrated lime at 2.5% of the total weight of aggregates generated an optimum improvement in the mechanical properties of the asphalt concrete mixes used for all three purposed layers (i.e., wearing, levelling, and base) at atmospheric temperatures from mild to relatively high. This paper reports on a continuous experimental test for the thermal properties of the optimized hydrated lime-modified mixes. The experiment together with that conducted before provides the required data to characterize the thermomechanical constitutive relations of the optimized hydrated lime-modified mixes. The obtained thermal and mechanical properties thereafter were implemented in a numerical modelling study for a scenario involving pavement exposed to coupled thermal and traffic service conditions. The study has demonstrated that using HL in mineral filler enhances the thermal properties of asphalt concrete, which, however, showed little influence on the local temperature profiles within the pavement structure. The thermal effect is pronounced under the coupled thermomechanical conditions for a pavement exposed to both traffic and climatic impacts. The HL pavement has about 1.5% less deformation, and 39% less stress level under traffic loading only, but the thermal effect increases the maximum total internal tensile stress level by 26% in the HL pavement in winter season. The modelling analysis has shown that the local maximum tensile stress dominates in the surface region of the HL pavement. It will help to reduce the workload of crack repairing and in long term help on saving costs and efforts of maintenance.

Keywords: asphalt concrete; thermal-mechanical coupling; pavement design



Citation: Al Ashaibi, A.; Wang, Y.; Albayati, A.; Byzyka, J.; Scholz, M.; Weekes, L. Thermal Properties of Hydrated Lime-Modified Asphalt Concrete and Modelling Evaluation for Their Effect on the Constructed Pavements in Service. *Sustainability* **2022**, *14*, 7827. <https://doi.org/10.3390/su14137827>

Academic Editors: Nuha Mashaan, Nur Izzi Md Yusoff and Saad Issa Sarsam

Received: 27 May 2022

Accepted: 23 June 2022

Published: 27 June 2022

Publisher's Note: MDPI stays neutral with regard to jurisdictional claims in published maps and institutional affiliations.



Copyright: © 2022 by the authors. Licensee MDPI, Basel, Switzerland. This article is an open access article distributed under the terms and conditions of the Creative Commons Attribution (CC BY) license (<https://creativecommons.org/licenses/by/4.0/>).

1. Introduction

Using hydrated lime (HL) as the mineral filler has been practiced on asphalt pavement concrete for a long time. So far, extensive laboratory studies and field tests have accumulated undisputable evidence and a large amount of data for its benefits on the obtained

mechanical properties of the asphalt concrete mixes and the performance and service life of their constructed pavements under a wide range of traffic loads and environmental conditions. The beneficial improvements of HL addition include significant reduction of the aging of the bitumen and increase of the resistance to permanent deformation (rutting), moisture damage, and thermal and fatigue cracking [1].

In spite of considerable research on HL-modified asphalt concrete, traditional research has primarily focused on the interest in mechanical properties under different temperature and environmental exposure conditions to identify the optimum rate of HL addition [2–4]. For example, a recent durability investigation on a pavement having five years of service showed that HL addition increased the resistance to moisture damage, but the differences between 0.5 and 1.5% HL addition were very limited [5]. Other experimental work in the laboratory showed that the utilization of HL as a filler at 2.5% content demonstrated a significant improvement on the resistance of the mixture to water, freezing, cracks from thawing [6]. Another previous laboratorial study has also reported that a partial replacement of a base limestone filler using 2.5% HL by total aggregate weight produced an optimum improvement on wider mechanical properties covering permanent deformation, fatigue life, and moisture susceptibility [3,7,8].

However, so far little research has been reported on the thermal properties of HL-modified asphalt concrete [9], although a better understanding of the thermal response of the HL-modified asphalt concrete is important and needs to be evaluated at the stage of pavement design [10–12]. To fill this gap, this paper first reports an experimental work conducted to determine the thermal properties of two types of asphalt concrete mixes with and without HL modification. Thereafter, the experimental results are implemented in numerical modelling to analyze the thermal and mechanical behavior of a pavement structure using asphalt concrete under a scenario of coupled traffic loading and environmental temperature variation. Both the experiment and modelling analysis have not only confirmed the benefits of the use of HL as the mineral filler for asphalt concrete, but also produced some initial data and novel work concerning the modelling methodology for the pavement and environment system.

2. Experiment

2.1. Raw Materials and Mixtures

The experiment is an extension of a previous study on the mechanical properties of HL-modified concrete [3] and was conducted in the same laboratory. The component materials, the asphalt cement, aggregates, and mineral fillers (limestone dust and hydrated lime) are the same as those in the previous study. The asphalt concrete samples were designed for the application of wearing, levelling, and base course, respectively, following the standard for road and bridge construction [13] for the types IIIA, II, and I. Two types of mixes were made for each specific layer application. One is the control mix, which used limestone dust only for the mineral filler, and the other is based on the control sample with partial replacement of the limestone filler using HL by 2.5% of the total weight of aggregate. The asphalt cement had a penetration grade of 40–50. The optimum asphalt content was determined using the Marshall test for all mixes (Table 1). The mineral filler content for the three types of applications are in the mid-range, which are 7%, 6%, and 5% of the total weight of the mixes for the wearing, levelling, and base course, respectively. All mixes used the same aggregate of a gradation, detailed in Table 2. The hydrated lime was added into the mixture of the aggregate and limestone filler in the form of dry powder.

Table 1. Optimum Asphalt Cement (OAC) Contents.

Notation	Application	Hydrated Lime Content (%)	OAC%
CW	Wearing	0	4.9
CL	Levelling	0	4.6
CB	Base	0	4.3
HL2.5W	Wearing	2.5	5.3
HL2.5L	Levelling	2.5	5
HL2.5B	Base	2.5	4.6

Table 2. Selected Gradations for Asphalt Concrete Mixtures with Specification Limits.

Sieve Size	mm	Type I	Type II	Type IIIA
		Base Course	Levelling Course	Wearing Course
		% Passing by Weight of Total Aggregate and Filler		
1.5 in	37.5	100		
1 in	25.0	95	100	
0.75 in	19.0	83	95	100
0.5 in	12.5	68	80	95
3/8 in	9.5	61	68	83
No. 4	4.75	44	50	59
No. 8	2.36	32	36	43
No. 50	300 μ m	11	12	13
No. 200	75 μ m	5	6	7

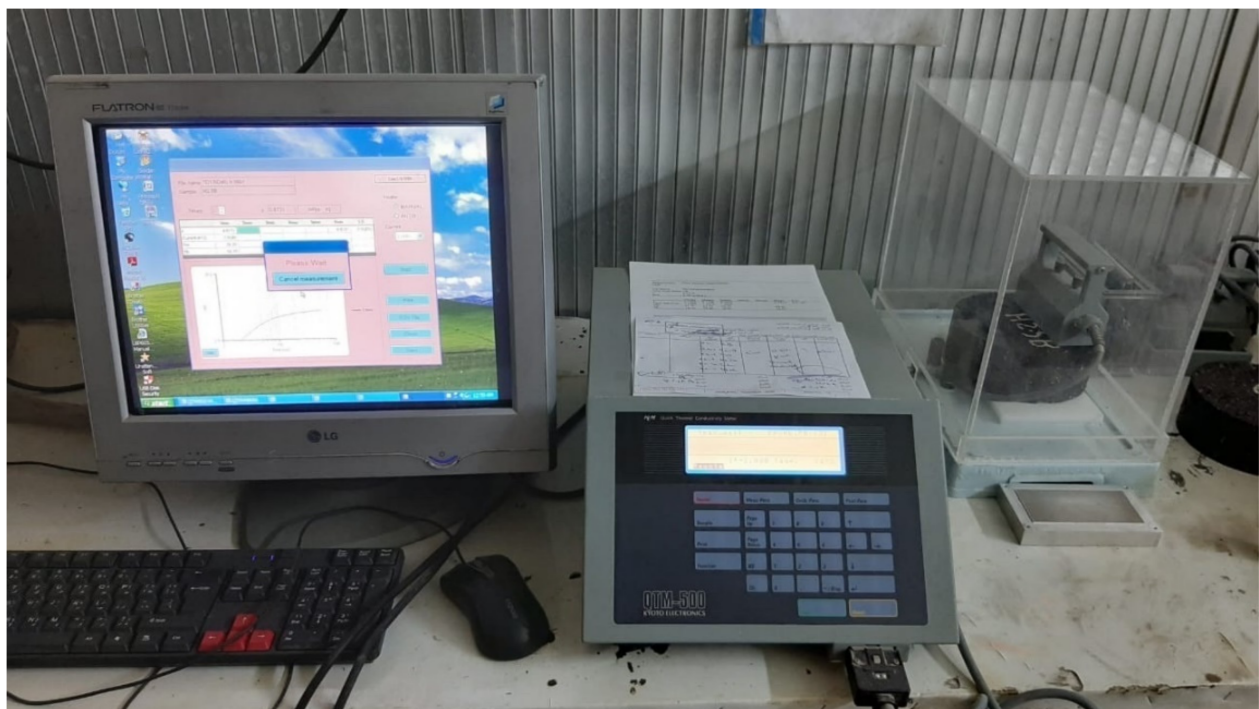
2.2. Specimen Preparation and Thermal Property Test

At first, the prepared aggregate of the added mineral filler and asphalt cement were separately placed in different trays, put in an oven, and heated to reach a uniform temperature of 160 °C. The asphalt cement was then mixed manually with the aggregate on a hot plate at the exact amount of the OAC given in Table 1. The prepared mixture was then loaded in a bowl and put back in an oven at a controlled temperature (150 °C for 10 min) before being cast and compacted in preheated cylindric molds to make the specimens for testing. The dimensions of the molds are 150 mm in diameter and 62.7 mm in height. The mixtures in the molds were compacted by 114 blows on each end using a hammer (weight of 4.536 kg) falling at a height of 457.2 mm. Finally, the prepared specimens were left to cool at room temperature for 24 h before conducting the test. Figure 1 illustrates the prepared raw materials, mixing procedure, and the specimens made. Samples were triplicated for each measurement.

The thermal properties were measured using the Quick Thermal Conductivity Meter QTM500 as shown in Figure 2. The QTM-500 probe contains a thermocouple and a heater. The temperature of the heater rises exponentially, which presents a linear trend with the heating time on a logarithmic scale as shown in Figure 2b. The specimen's thermal conductivity (λ) is calculated in terms of the slope of the linear trend according to the formula shown in the Figure 2b.



Figure 1. The mixing procedure and the made specimens.



(a)

Figure 2. Cont.

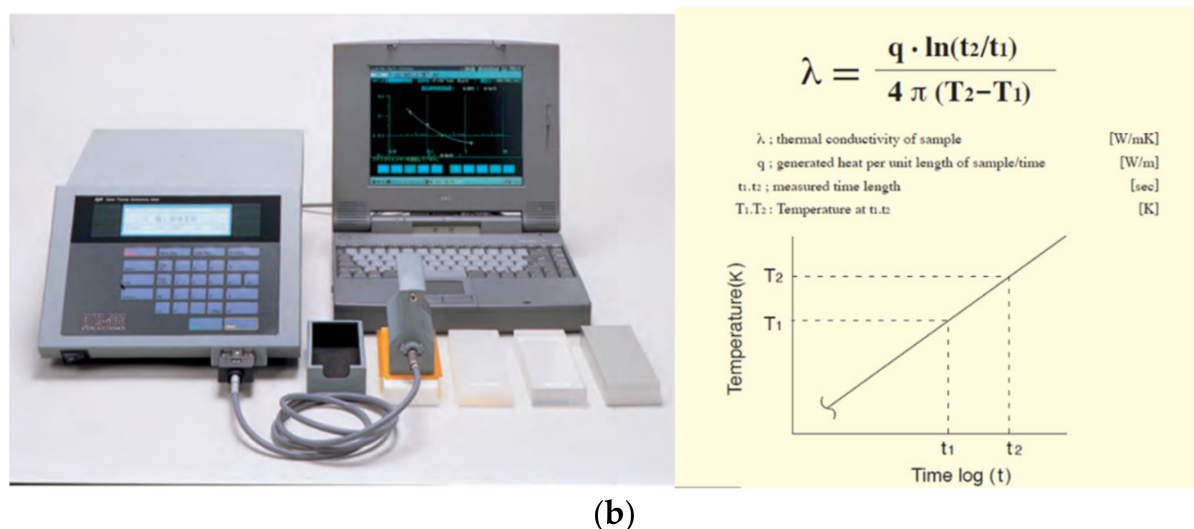


Figure 2. Thermal property test. (a) Experiment setup. (b) The principle for parameter measurement.

2.3. The Experimental Results

Figure 3 compares the measured bulk density and two thermal properties between the control mixes and that of 2.5% HL addition. It can be seen that HL addition has a very small influence on the bulk density, but significantly increases the thermal conductivity and thermal capacity (specific heat). Specifically, the increase in thermal conductivity is 27% for the wearing mix, 7% for the leveling mix, and 17% for the base mix. The increase in specific heat is 25% for the wearing mix, 6% for the leveling mix, and 16% for the base mix. Theoretically, a high magnitude of thermal properties will help crack healing. An interesting finding is that for both the control and the 2.5% HL specimens, the OAC and the filler content decreased from the wearing, through the levelling, to the base course application. However, while the thermal properties present a steady increase for the three control mixes, for the 2.5% HL mixes, levelling specimens show the lowest value for the two thermal properties. This means that there is no single correlation of the thermal properties with either the optimized asphalt cement or the mineral filler content.

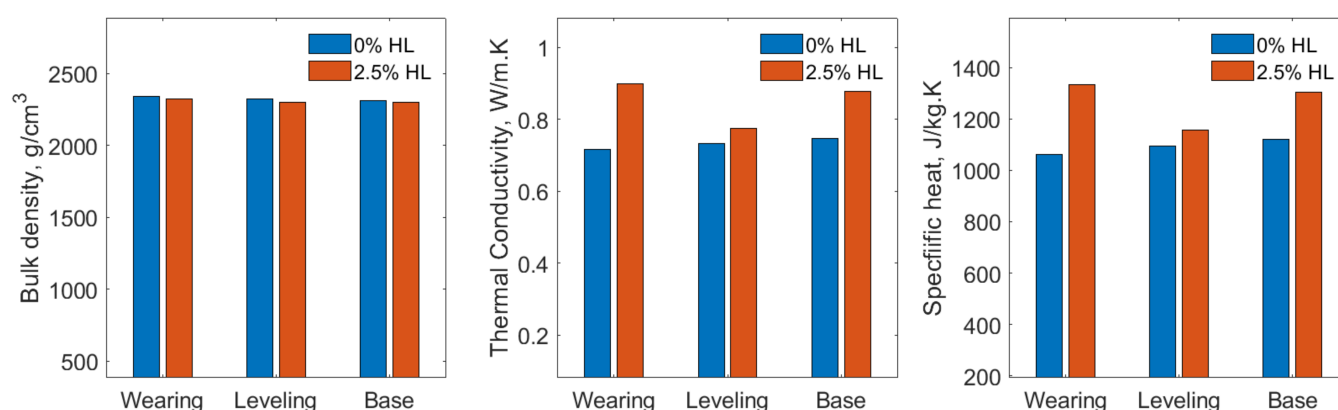


Figure 3. Comparison of the thermal properties between the control mix and the mix of 2.5% hydrated lime.

3. Modelling Evaluation for the Pavement Constructed Using HL Asphalt Concrete

A finite element modelling analysis was conducted to evaluate the benefit for a pavement structure using the HL-modified asphalt concrete under a service scenario exposed to a condition coupling a traffic loading and a typical seasonal temperature variation experienced in the UK. A classical thermomechanical model [14] was adopted, which establishes a motion equation and thermal energy conservation as briefed below:

- Motion equation

For an isotropic solid material, its deformation follows the Navier's equations, which can be written in the form below Equation (1):

$$\frac{E}{2(1+\nu)} \left(\frac{1}{(1-2\nu)} \nabla(\nabla \cdot \mathbf{u}) + \nabla^2 \mathbf{u} \right) + \mathbf{f} = \rho \quad (1)$$

where \mathbf{u} stands for the vector of displacement in space ($u_x; u_y; u_z$), \mathbf{f} is a body force per unit volume, E is modulus, ν is the Poisson ratio, and ρ is density. The strain and stress of the solid material are shown in Equations (2) and (3), respectively.

$$\varepsilon_{ij} = \frac{1}{2} \left(\frac{\partial u_i}{\partial x_j} + \frac{\partial u_j}{\partial x_i} \right) \quad (2)$$

$$\sigma_{ij} = \lambda \varepsilon_{kk} \delta_{ij} + 2\mu \varepsilon_{ij} - \alpha(3\lambda + 2\mu) \Delta T \delta_{ij} \quad (3)$$

where $\lambda = \frac{\nu E}{(1-2\nu)(1+\nu)}$ and $\mu = \frac{E}{2(1+\nu)}$ are the Lamé parameters, α is the thermal expansion/contraction coefficient, and ΔT is the temperature change, which, in the modelling work of this paper, is linked to a reference temperature of 10 °C for the scenario of the UK climate.

- Energy equation

When exposed to a heat transfer process, the solid material satisfies the thermal energy conservation condition as shown in Equation (4).

$$\rho c_p \frac{dT}{dt} = \nabla(k \nabla T) + \rho r - \alpha(3\lambda + 2\mu) T \frac{d\varepsilon_{kk}}{dt} \quad (4)$$

where c_p is the specific heat, k is the thermal conductivity, and r is the heat source per unit mass. For the pavement challenge, the heat source r and the thermal energy, due to the deformation strain rate ($\frac{d\varepsilon_{kk}}{dt}$), are neglected in this study.

Equations (1)–(4) closely describe the thermomechanical state of a structural system. They were applied to analyze a pavement structure of three asphalt layers using the mixes investigated in the experiment described above. Figure 4 illustrates a constructed five-layer single carriageway pavement structure. Finite element analysis (FEA) modelling was conducted for half of the symmetric structure. A wheel pressure was applied on the surface representing traffic loading. The geometric information has been presented in Table 3. The traffic load was set at a scenario of an equivalent single wheel load of 70 kN referring to a statistic traffic condition (Table A1). The load magnitude, which gives a wheel load pressure of 0.772 MPa on an estimated contact area of $9.073 \times 10^{-2} \text{ m}^2$ [7], was deliberately increased for this study in terms to compare with the thermal effect. The Equations (1)–(4) were solved using the partial differential equation module of a commercial FEA software (COMSOL Multiphysics).

Table 3. Finite element geometric data.

	Surface/Wearing	Binder/Levelling	Base	Subbase	Subgrade	Wheel
Thickness (mm)	50	70	90	300	2500	-
Width (mm)	1800	1800	1800	1800	1800	250

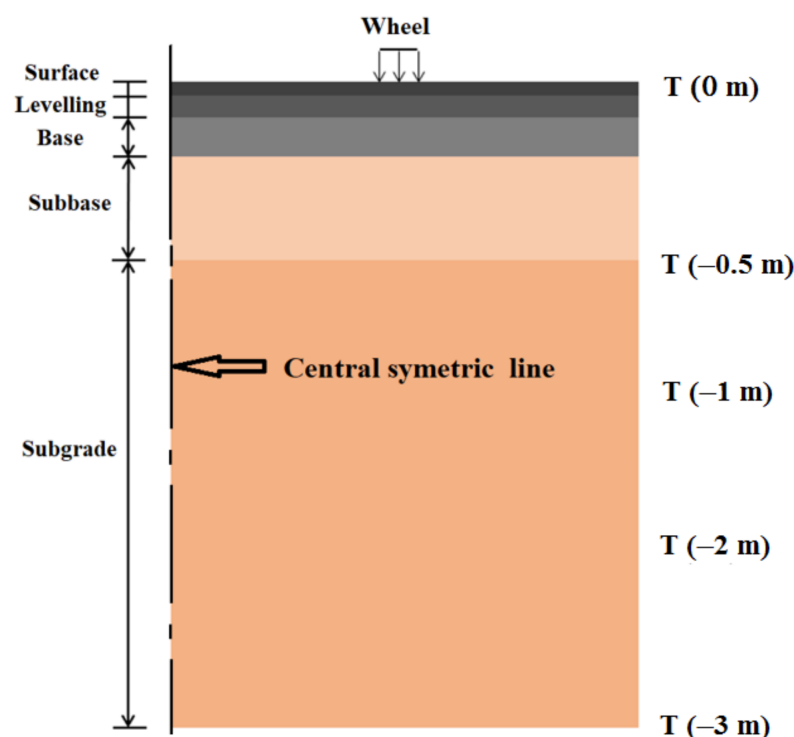


Figure 4. FE geometric model.

Table 4 lists the mechanical properties of the mixes of three pavement layers, which were reported in a previous study [3], and the thermal properties from this study. The data for the two foundation layers (subbase and subgrade) refer to another published work [15]. A thermal deformation model based on a laboratory study on a newly constructed asphalt pavement [16] was adopted to estimate the bulk material temperature effect on the coefficient of thermal expansion (CTE) and contraction (CTC). They are two quadratic polynomials in the form of the Equation (5).

$$CTC = -1.62 \times 10^{-8}T^2 + 9.46 \times 10^{-7}T + 1.75 \times 10^{-5} \quad (5a)$$

$$CTE = 4.34 \times 10^{-9}T^2 - 2.34 \times 10^{-7}T + 2.78 \times 10^{-5} \quad (5b)$$

Table 4. Material Properties for Finite Element Analysis.

Property	Mix	Wearing	Levelling	Base	Subbase	Subgrade
Modulus * E (MPa)	0% HL	$0.28T^2 - 41.53T + 2090$	$0.39T^2 - 46.41T + 1929$	$0.34T^2 - 40.41T + 1649$	170	65
	2.5% HL	$0.19T^2 - 43.03T + 2623$	$0.52T^2 - 63.3T + 2527$	$0.34T^2 - 41.12T + 1803$	170	65
Poisson ratio ν	0% HL		0.35			
	2.5% HL					0.4
Density ρ (g/cm ³)	0% HL	2.34	2.32	2.31		
	2.5 HL	2.32	2.30	2.3	1.76	1.29
Thermal Conductivity k (W/m/K)	0% HL	0.71	0.73	0.75		
	2.5 HL	0.90	0.78	0.88	1.3	0.28
Thermal Capacity c_p (J/kg/K)	0% HL	1062.6	1092.79	1121.12		
	2.5 HL	1333.48	1155.49	1303.09	837	800
Thermal deformation coefficient * α	0% HL		CTC—Equation (5a)			
	2.5 HL		CTE—Equation (5b)		3.32×10^{-6}	3.4×10^{-5}

* The temperature in the relevant formula has the unit °C.

The thermal interaction between the pavement and the atmospheric environment is a complex process dominated by the heat transfer in the forms of conduction, radiation, and convection at the pavement surface and surrounding ground conditions. Under special climatic conditions, other physics such as the latent heat flux due to ice melting or moisture

evaporation is involved as well [17]. The heat exchange mechanism in the pavement–climate system has been topical research for a long time [18]. Characteristic models for the details of the underlining physics have been proposed and developed [19–21]. In this paper, the UK climate and environment are set as a scenario for the modelling case study. As the primary purpose is to evaluate the effect of HL-modified asphalt concrete on pavement behavior, a simplified Dirichlet temperature boundary condition is adopted for the pavement structure based on a geological survey on the shallow ground seasonal temperature in the UK [22].

Figure 5 shows a characterization model using a sine function to fit the shallow ground temperature variation at five depths, i.e., 0, −0.5, −1, −2, and −3 m. The data are from reference [22]. Figure 5 provides temperature variation information by days. However, the daily weather temperature change in the UK, in general, would be about 10 °C for a year-round time. Based on this assumption, a daily weather temperature variation is assumed to take a sine wave form in a 24 h period, and is embedded in the data curves of Figure 5 as shown by Figure 6a. Combining the daily weather temperature variation with the yearly variation curve for 0 m depth, an annual pavement surface temperature variation by hours is shown in Figure 6b,c.

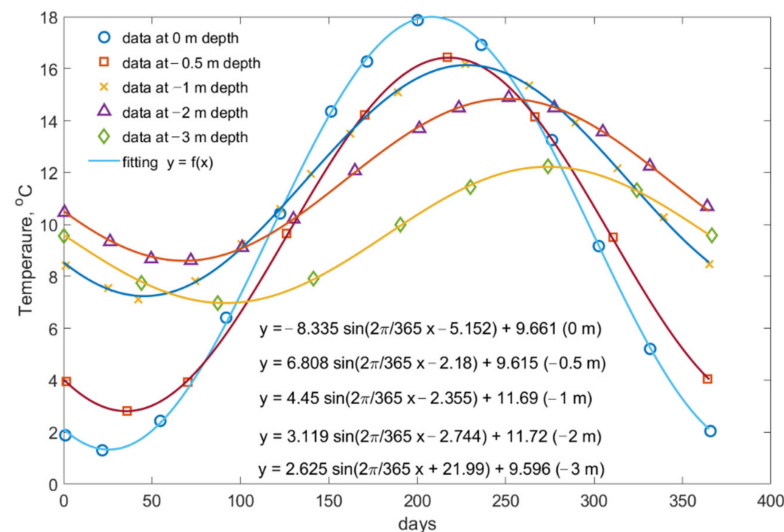


Figure 5. Characterization modelling for year-round UK shallow ground temperature variation.

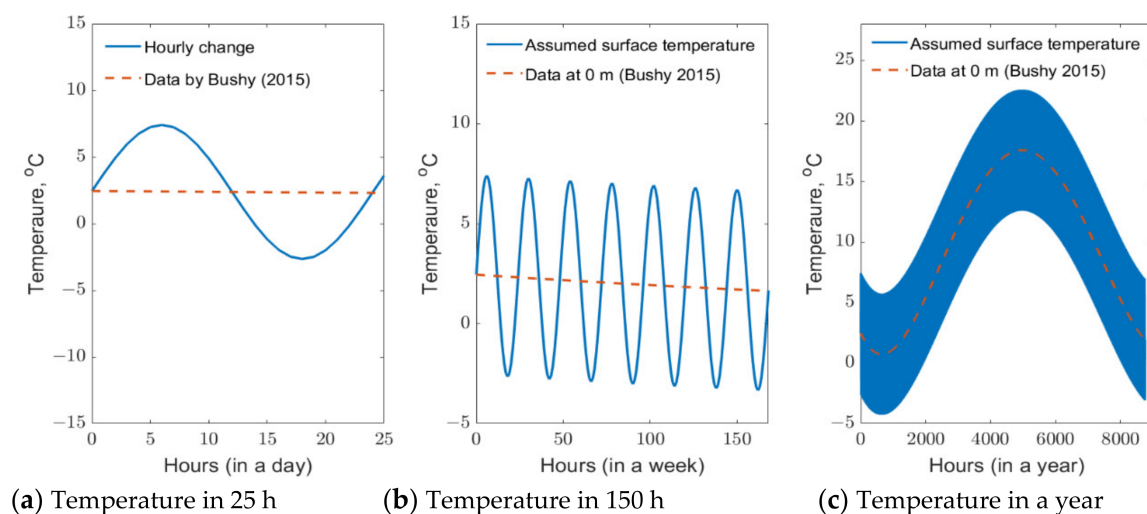


Figure 6. The assumed seasonal temperature condition at the pavement surface.

The pavement surface temperature was set to be the seasonal temperature at a depth of 0 m, i.e., $T(0\text{ m})$. The bottom surface temperature was set to be $T(-3\text{ m})$. The other boundary conditions are a thermal isolation along a left symmetric vertical line and the temperature of the right vertical edge, which is interpolated according to the annual below-ground temperature variation data using the fitting curves in Figure 5b at the corresponding depth illustrated in Figure 4. It also assumes that there is no horizontal displacement for the vertical edges of all layers and no vertical displacement at the bottom of the subgrade. An initial temperature condition in the whole structure is assumed to have a value of $8.7\text{ }^{\circ}\text{C}$, the mean value of the seasonal temperature at the depth -0.5 m , when solving the energy equation, Equation (4).

4. Modelling Results and Discussion

4.1. Temperature Profile and Thermal Strain & Stress Distribution

Numerical computing was performed at an hourly time step starting from the 0 h on the 1st day in January. Figure 7 shows the temperature profile at the time in four typical seasons. The modelling time of 720 h occurred in February, 2880 h in May, 5040 h in August, and 7200 h in November. It can be seen that the annual temperature variation degree in pavement decreases with the depth downward. February and August have a big temperature variation from the top of wearing course to the bottom of subgrade. May and November have a small vertical temperature variation. The wearing course has the highest temperature variation gradient all year round.

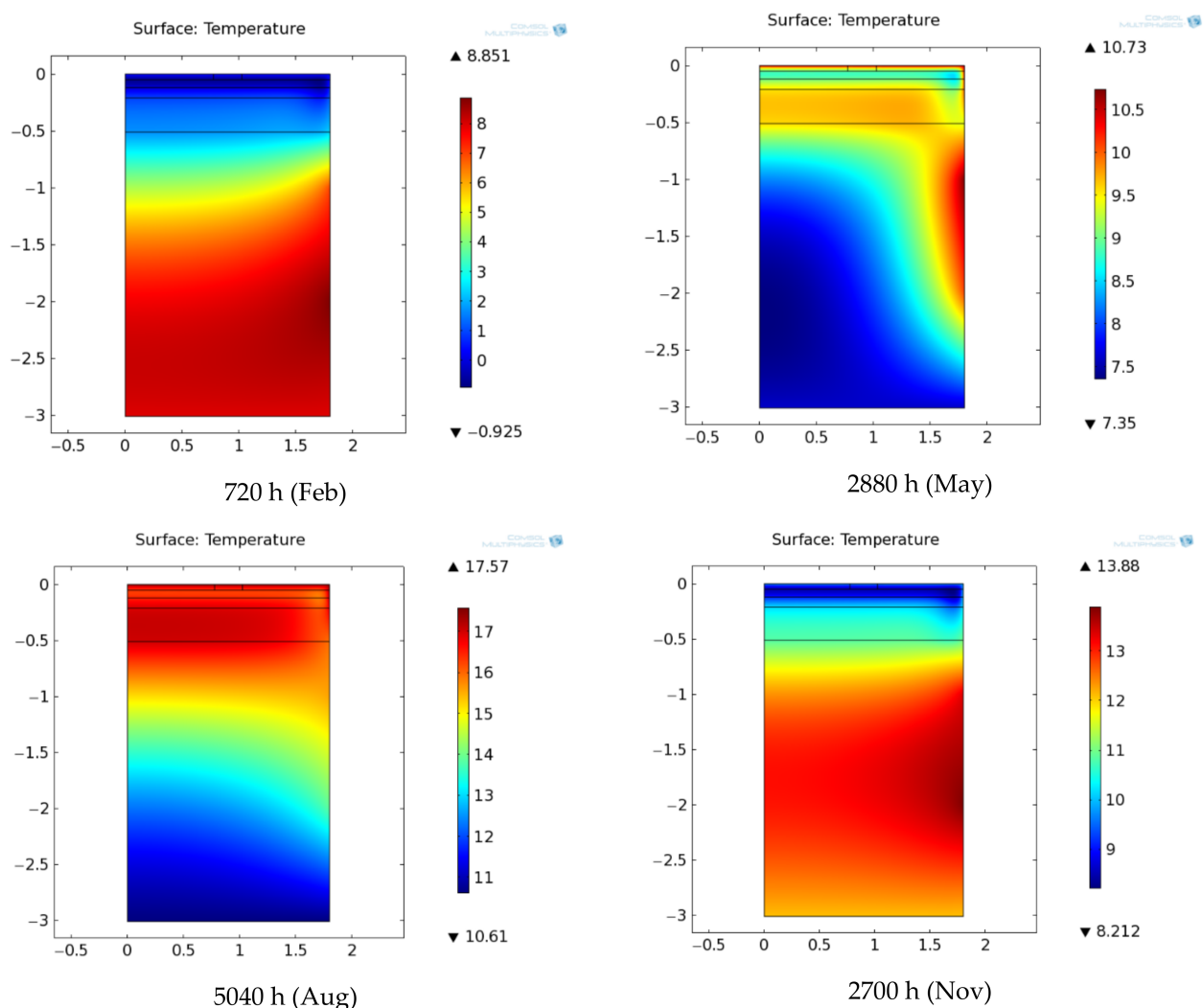


Figure 7. The seasonal temperature profile in the pavement structure.

Figure 8 compares the vertical temperature distribution along the central symmetric line (Figure 4) between the pavements of 2.5% HL and 0% HL. It shows that although the HL-modified asphalt concrete narrows the temperature variation range along the three asphalt layers and the subbase, particularly in the season of February, the difference is very small. The highest local temperature difference is less the 1 °C at wearing layer.

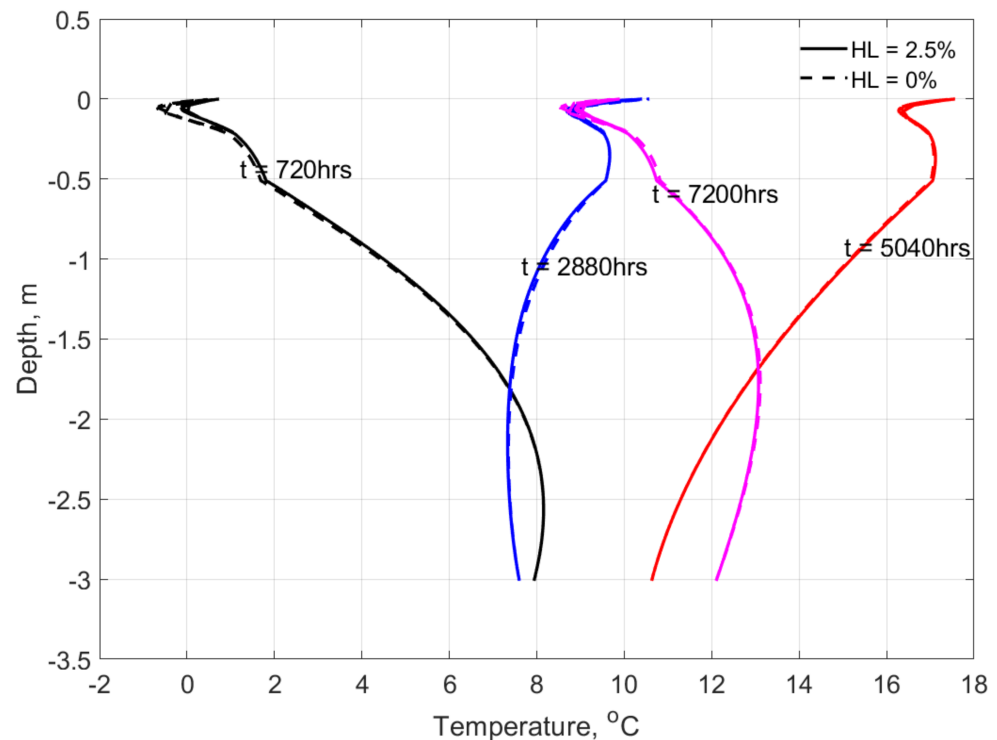


Figure 8. The vertical temperature profile along the symmetric centre of pavement.

Figure 9 shows the vertical distribution of the thermal strain ($\alpha\Delta T$) and stress ($\alpha(3\lambda + 2\mu)\Delta T$) along the central symmetric line. It can be seen that the highest inconsistent thermal strain exists at the interface between the subbase and the subgrade. However, the biggest thermal stress happens at the surface of the wearing course.

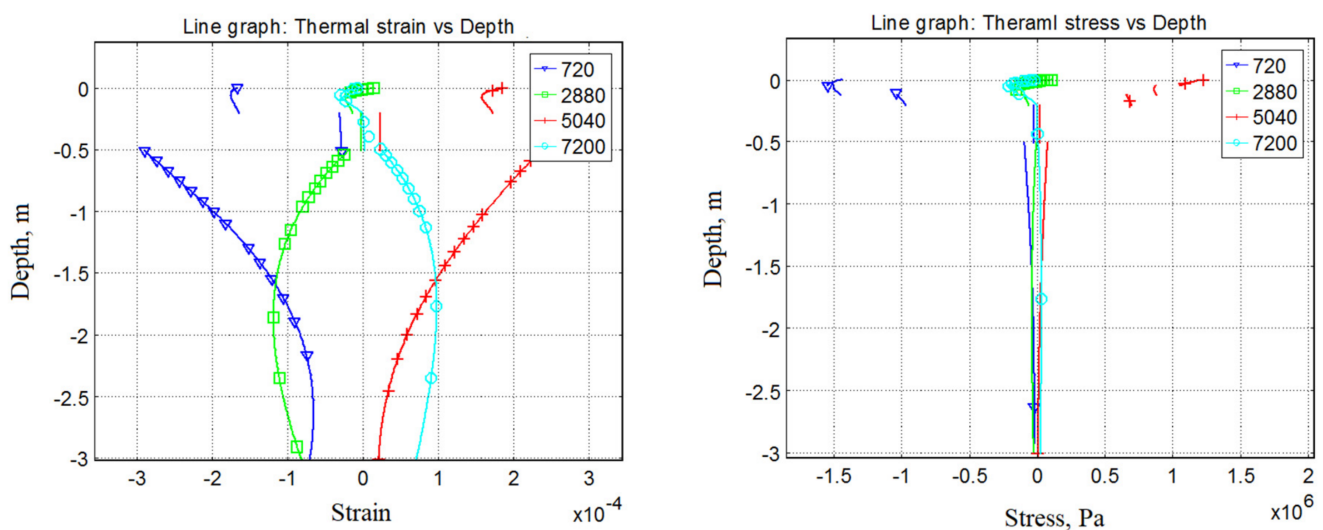


Figure 9. The thermal strain and stress in 2.5%HL pavement.

4.2. The Coupled Thermomechanical Effect

Figure 10 compares the vertical of the pavement surface under a coupled thermomechanical situation. It shows that the pavements of 2.5% HL and 0% HL are very similar in the response to the environmental temperature variation. However, the HL pavement has less vertical deformation in all year-round under traffic loading. In the center of the pavement ($x = 0$), under the coupled thermomechanical condition, pavement using no HL has a higher vertical displace at all four times. Comparing the maximum vertical displacement at the position of the wheel load, the 2.5% HL pavement is about 1.5% less than that of the control 0% HL pavement. The result highlights the benefit of HL on the long-term fatigue life and rutting of the pavement under repetitive loads.

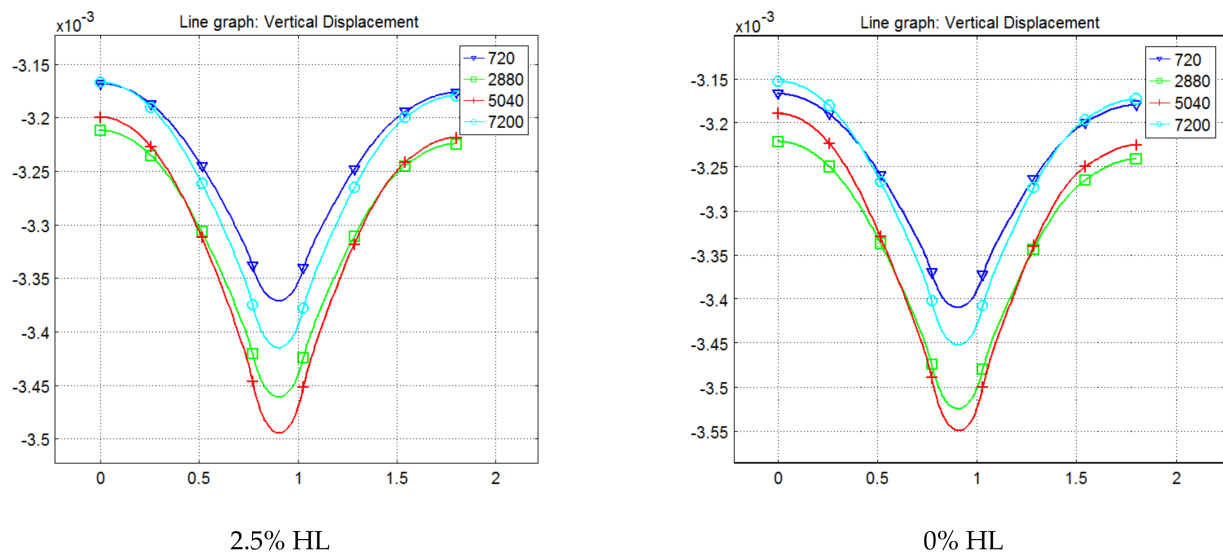


Figure 10. Vertical displacement of the Pavement Surface.

Figure 11 shows the sum of the two principal stresses, in Equation (6), due to traffic loading. It is undisputable that the maximum value is in the wearing course at the edge of the contact region with wheels. It can be seen that the traffic stress is dominant in the three layers of the asphalt pavement

$$\sigma_{max/min} = \frac{\sigma_{xx} + \sigma_{yy}}{2} \pm \sqrt{\left(\frac{\sigma_{xx} - \sigma_{yy}}{2}\right)^2 + (\tau_{xy})^2} \quad (6)$$

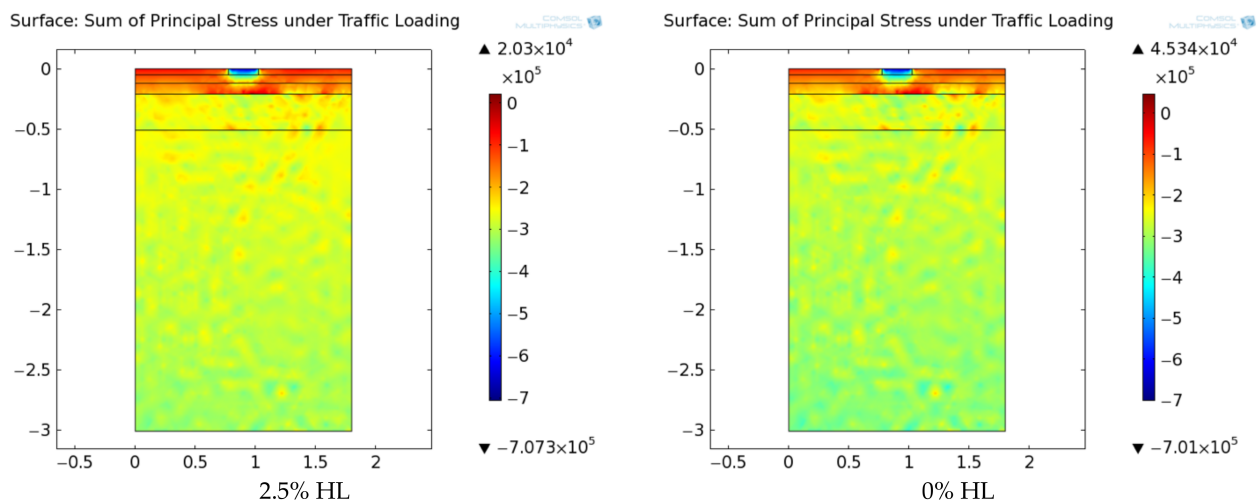


Figure 11. Sum of the 1st and 2nd principal traffic stress at time 720 h.

Figure 12 compares the maximum value of the sum of the two principal traffic stresses, and the maximum coupled stress of the sum of the two principal traffic stresses and the thermal stress for a year-round time. Referring to Equation (3), the coupled stress ($s_{p1}+s_{p2}-s_T$ in the legend) is defined as: $\sigma_{max} + \sigma_{min} - \alpha(3\lambda + 2\mu)\Delta T$. It shows that the HL pavement has a less internal stress level under traffic loading only. However, the thermal effect, particularly at low temperature (during the winter season), causes more internal tensile stress level in the HL pavement than in the pavement with no HL. In the two pavement structures, the thermal effect outweighs the traffic effect in the time of winter season between 0~2500 h and 7500 h to the end of the year. The maximum sum of the principle traffic stress is 0.17 MPa at 5000 h and the maximum couple stress is 1.46 MPa at about 720 h for the HL pavement, while the two maximum values for the control pavement are 0.28 MPa and 1.15 MPa. The results indicate that the benefit of HL on only traffic stress reduction is about 39%, but the thermal effect on the maximum internal tensile stress is 26% higher in the HL pavement. This result explains why there is an optimum content of HL for asphalt concrete modification when exposed to temperature variation [2] (Al-Tameemi et al. 2016).

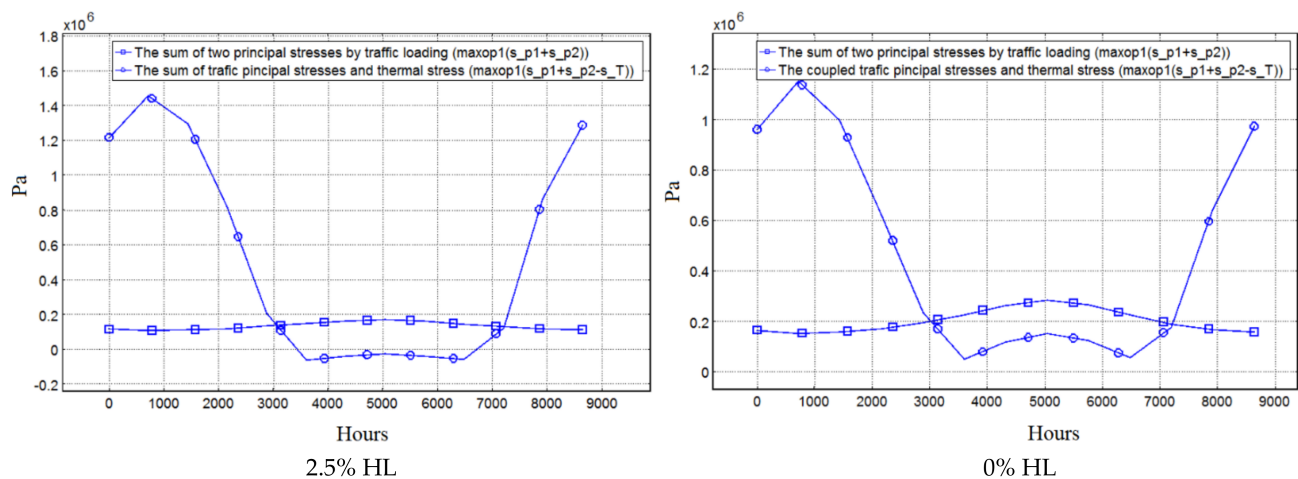


Figure 12. Maximum stress value in the pavement in year round.

Figure 13 shows the coupled stress ($\sigma_{max} + \sigma_{min} - \alpha(3\lambda + 2\mu)\Delta T$) profile in pavement at the time of 720 h in winter season. For HL pavement, the highest tensile stress is located predominantly in the wearing course, while for the pavement of no HL, high tensile stress is not only located in the wearing course but also at the bottom of the base course.

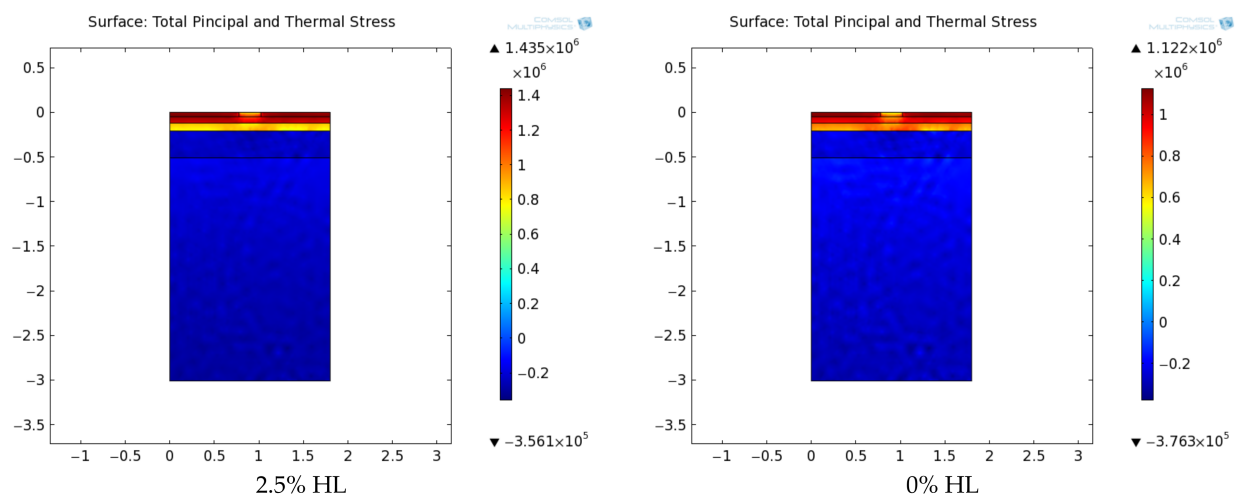


Figure 13. The coupled thermomechanical stress, $\sigma_{max} + \sigma_{min} - \alpha(3\lambda + 2\mu)\Delta T$, at 720 h.

5. Conclusions

This paper reports on an experimental study on the thermal properties of asphalt concrete with added hydrated lime mineral filler. Thereafter, a numerical modelling was conducted to analyze the environmental thermal influence and the coupled thermomechanical effect on the behavior of the constructed pavement structures. The following can be drawn from this study.

- 2.5% addition of HL to replace the equivalent weight of limestone dust filler enhances the thermal properties of the modified asphalt concrete of increased magnitudes of thermal conductivity (27% for wearing mix, 7% for leveling mix, 0.17% for base mix) and specific heat (25% for wearing mix, 6% for leveling mix, 0.16% for base mix). For the HL modified mix there is no correlation between the thermal properties and either the optimum asphalt cement or the mineral filler content.
- Between pavement using HL concrete and that not using HL concrete, there is a very small difference between the local temperature profiles within the structural layers. Correspondingly, the difference of the thermal strain and stress profiles within the two pavements is very small as well.
- The thermal effect is pronounced under the coupled thermomechanical conditions for pavement exposed to both traffic and climatic impacts because of the temperature effect on the mechanical properties, such as the modulus and deformation coefficient, of the mixes.
- The modelling analysis shows that the HL pavement has about 1.5% less deformation than the control pavement at the place under the direct traffic loading. The result highlights the benefit of HL on long-term fatigue and rutting resistance.
- The modelling results indicate that the benefit of the HL on traffic-only stress reduction is about 39%, but the thermal effect increases that maximum total internal tensile stress level by 26% in the HL pavement in the winter season. It explains why there is an optimum HL content for asphalt concrete modification when exposed to temperature variation.
- The modelling results have showed that for HL pavement asphalt concrete, the local maximum tensile stress predominates in the surface region, i.e., wearing layer. It will help reduce the workload in crack repairing and in the long term help on saving costs and efforts of maintenance.

Author Contributions: Formal analysis, Y.W., A.A., J.B. and M.S.; Investigation, A.A.A. and A.A.; Methodology, A.A.A. and L.W.; Supervision, M.S.; Validation, Y.W. and L.W.; Writing—original draft, A.A.A.; Writing—review & editing, Y.W. and A.A. All authors have read and agreed to the published version of the manuscript.

Funding: This research is funded by a Ph.D. studentship sponsored by the government of Libya.

Institutional Review Board Statement: Not applicable.

Informed Consent Statement: Not applicable.

Data Availability Statement: Not applicable.

Conflicts of Interest: The authors declare no conflict of interest.

Appendix A

Table A1. Traffic load information for estimating the 80-kN ESAL [7] (Al-Tameemi et al., 2019).

Vehicle Type	Percentage of ith Vehicles P_i (%)	Number of Vehicles/Lane per Year N_i	Equivalent Axle Load Factor (EALF)	Growth Factor G_f	ESALs
Passenger car unit (PCU)	55	250,937.50	0.0008	20.02	4019.02
Single-unit trucks					
2 axles, 4 tires	10	45,625	0.003	20.02	2740.24
2 axles, 6 tires	10	45,625	0.21	20.02	191,816.60
3 axles or more	5	22,812.58	0.61	20.02	278,590.80
Tractor semitrailers and combinations					
4 axles or fewer	5	22,812.50	0.62	20.02	283,157.90
5 axles	10	45,625	1.09	20.02	995,619.60
6 axles or more	5	22,812.50	1.23	20.02	561,748.70
Total	100	456,250			2,317,693

References

- Petersen, J.C. *A Review of the Fundamentals of Asphalt Oxidation: Chemical, Physicochemical, Physical Property, and Durability Relationships*; Transportation Research Circular; Transportation Research Board: Washington, DC, USA, 2009; 78p.
- Al-Marafi, M.N. Effects of Hydrated Lime on Moisture Susceptibility of Asphalt Concrete. *Adv. Sci. Technol. Res. J.* **2021**, *15*, 13–17. [\[CrossRef\]](#)
- Al-Tameemi, A.F.; Wang, Y.; Albayati, A. Experimental Study of the Performance Related Properties of Asphalt Concrete Modified with Hydrated Lime. *J. Mater. Civ. Eng.* **2016**, *28*, 04015185. [\[CrossRef\]](#)
- Iwanski, M.M. Effect of Hydrated Lime on Indirect Tensile Stiffness Modulus of Asphalt Concrete Produced in Half-Warm Mix Technology. *Materials* **2020**, *13*, 4731. [\[CrossRef\]](#) [\[PubMed\]](#)
- Bourona, S.; Hammouma, F.; Ruatb, H.; Métaisc, P.; Lesueur, D. Improving the durability of asphalt mixtures with hydrated lime: Field results from highway A84. *Case Stud. Constr. Mater.* **2021**, *14*, e00551. [\[CrossRef\]](#)
- Al-Bayati, H.K.A.; Oyeyi, A.G.; Tighe, S.L. Experimental Assessment of Mineral Filler on the Volumetric Properties and Mechanical Performance of HMA Mixtures. *Civ. Eng. J.* **2020**, *6*, 2312–2331. [\[CrossRef\]](#)
- Al-Tameemi, A.F.; Wang, Y.; Albayati, A. Moisture Susceptibility and Fatigue Performance of Hydrated Lime-Modified Asphalt Concrete: Experiment and Design Application Case Study, Journal of Materials in Civil Engineering. *Am. Soc. Civ. Eng.* **2019**, *31*, 4019019.
- Albayati, A.; Wang, Y.; Haynes, J. Size effect of hydrated lime on the mechanical performance of asphalt concrete. *Materials* **2022**, *15*, 3715. [\[CrossRef\]](#) [\[PubMed\]](#)
- Mirzanamadi, R.; Johansson, P.; Grammatikos, S.A. Thermal properties of asphalt concrete: A numerical and experimental study. *Constr. Build. Mater.* **2018**, *158*, 774–785. [\[CrossRef\]](#)
- Han, D.G.; Zhu, H.; Li, L.L. Dynamic simulation analysis of the tire-pavement system considering temperature fields. *Constr. Build. Mater.* **2018**, *171*, 261–272. [\[CrossRef\]](#)
- Li, Y.; Liu, L.; Sun, L. Temperature predictions for asphalt pavement with thick asphalt layer. *Constr. Build. Mater.* **2017**, *160*, 802–809. [\[CrossRef\]](#)
- Albayati, A.H.; Mohammed, A.M. Effect of Lime Addition Methods on Performance Related Properties of Asphalt Concrete Mixture. *J. Eng.* **2016**, *22*, 1–20.
- SCRB/R9-State Corporation of Roads and Bridges. *General Specification for Roads and Bridges*; Ministry of Housing and Construction: Baghdad, Iraq, 2003.
- Little, D.N.; Allen, D.H.; Bhasin, A. *Modeling and Design of Flexible Pavements and Materials*; Springer International Publishing AG: Cham, Switzerland, 2018.
- Ishikawa, T.; Miura, S. Influence of moving wheel loads on mechanical behavior of submerged granular road bed. *Soils Found.* **2015**, *55*, 242–257. [\[CrossRef\]](#)
- Islam, R.; Tarefder, R.A. Coefficients of Thermal Contraction and Expansion of Asphalt Concrete in the Laboratory. *J. Mater. Civ. Eng.* **2015**, *27*, 04015020-1. [\[CrossRef\]](#)
- Chen, J.; Wang, H.; Xie, P.-Y. Pavement temperature prediction: Theoretical models and critical affecting factors. *Appl. Therm. Eng.* **2019**, *158*, 113755. [\[CrossRef\]](#)
- Qiao, Y.-N.; Dawson, A.R.; Parry, T.; Flintsch, G.; Wang, W.-S. Flexible Pavements and Climate Change: A Comprehensive Review and Implications. *Sustainability* **2020**, *12*, 1057. [\[CrossRef\]](#)

19. Qin, Y.; Hiller, J.E. Modeling the temperature and stress distributions in rigid pavements: Impact of solar radiation absorption and heat history development. *KSCE J. Civ. Eng.* **2011**, *15*, 1361–1371. [[CrossRef](#)]
20. Qin, Y.-H. Pavement surface maximum temperature increases linearly with solar absorption and reciprocal thermal inertial. *Int. J. Heat Mass Transf.* **2016**, *97*, 391–399. [[CrossRef](#)]
21. Wu, H.; Sun, B.; Li, Z.; Yu, J. Characterizing thermal behaviors of various pavement materials and their thermal impacts on ambient environment. *J. Clean. Prod.* **2018**, *172*, 1358–1367. [[CrossRef](#)]
22. Busby, J. UK shallow ground temperatures for ground coupled heat exchangers. *Q. J. Eng. Geol. Hydrogeol.* **2015**, *48*, 248–260. [[CrossRef](#)]